Improving the Thermal Condition of the High-Pressure Turbine Blade

V. M. Zubanov[a], G. M. Popov[b], S. A. Melnikov[c] , A. I. Sherban[d] and Liu Xin[e]
Department of Aircraft Engine Theory, Samara National Research University,
34 Moskovskoe Highway, Samara, Russian Federation

Keywords: Aircraft Engine, Turbine Cooling, Cooled Blades, Cooling Efficiency Coefficient.

Abstract: An increase in the temperature of the gases forces the cooling system of the turbine blades to become more and more complex. The presented article describes a complex and computer-intensive numerical model of a working blade of a modern high-pressure turbine of a civil aviation aircraft gas turbine engine, which includes a flow region, a blade body, internal cooling channels and coolant supply channels. Using this model, the thermal state of the blade was determined and potential problem areas were found: hot gas leakage, coolant stagnation and overheating. Based on the analysis, several options were proposed for changing the configuration of the internal channels of the blade, which reduce the negative effects found. Although the proposed design options did not fully achieve all the requirements for the blade, they made it possible to find promising ways for further improvement. Also, the authors have practically worked out conjugate numerical models to study the thermal state of the turbine.

1 INTRODUCTION

The operation of modern gas turbine engines (GTE) is impossible without a cooling system for high-temperature gas turbine components. Therefore, the turbine cooling system includes cooling of the nozzle blades (NB) and rotor wheels (RW). The cooling schemes for the NB and RW in the first stage of a high-pressure turbine (HPT) are the most complex. They must ensure a component temperature at which the turbine can operate effectively throughout its full service life, bearing in mind that the total working fluid temperature at the combustion chamber outlet T_g^* can exceed 1800 K in modern engines (Han J.C.,2012, Inozemtsev A.A., 2006).

Different schemes of cooling air channels, which contain heat exchange intensifiers, are used to cool the HPT rotor blades (Kopelev S.Z., 1983, Nagoga G.P.,1996, Vieser, W., 2002). The design of effective blade cooling schemes is a time-consuming process, which is currently difficult to imagine without the use of CFD tools.

The purpose of this work was to perform a detailed analysis of the thermal condition of the cooled HPT rotor blade (RB) using the Ansys CFD Post software, and to develop and implement measures to improve the thermal condition of the blade and increase the efficiency of its cooling scheme.

In the course of this work, alternative schemes of internal cooling channels were developed based on the analysis of the thermal condition of the HPT rotor blades. Geometric models of the blade under study were created with preservation of the external shape and different schemes of internal cooling channels. Using these models, several series of calculations were carried out. The results of various cooling schemes have been compared with each other in order to assess the effect of changes in the HPT rotor blades cooling scheme on its temperature condition.

[a] https://orcid.org/0000-0003-0737-3048
[b] https://orcid.org/0000-0003-4491-1845
[c] https://orcid.org/0000-0002-0170-3846
[d] https://orcid.org/0000-0001-6699-3541
[e] https://orcid.org/0000-0002-3137-8247

Zubanov, V., Popov, G., Melnikov, S., Sherban, A. and Xin, L.
Improving the Thermal Condition of the High-Pressure Turbine Blade.
DOI: 10.5220/0012078400003546
In *Proceedings of the 13th International Conference on Simulation and Modeling Methodologies, Technologies and Applications (SIMULTECH 2023)*, pages 234-242
ISBN: 978-989-758-668-2; ISSN: 2184-2841

2 COMPUTATIONAL MODEL PREPARATION

As the initial data, the results of calculation of the thermal condition of the initial variant of the HPT RB cooling scheme were used. This cooling scheme is referred to hereinafter as the "basic" one, since modified cooling channels schemes were created based on it. The geometric model of the "basic" blade and its inner cavity is shown in Figure 1.

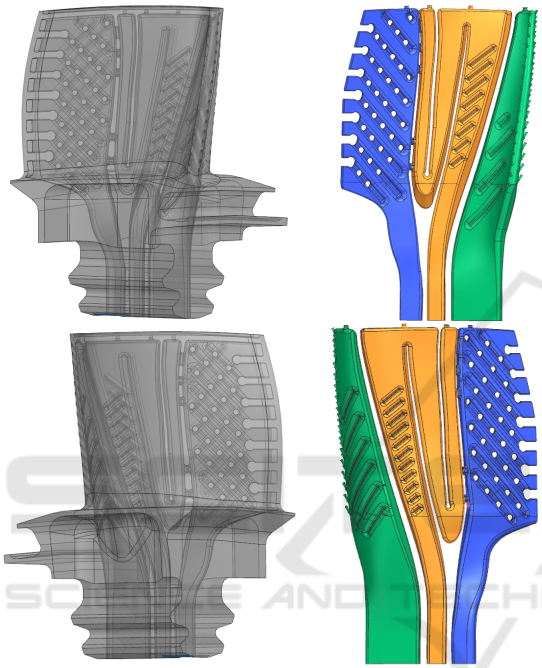

Figure 1: Shape of the basic rotor blade and its inner cavity.

Three-dimensional geometric models of the blade and gas-air regions were created in the Siemens NX software package. The RB inner cavity had a complex system of channels and included different types of convective cooling intensifiers, shown in Figure 2.

The blade has a total of three internal channels: front, middle and rear. The rear part of the blade is cooled by means of a vortex cooling matrix formed by crossed ribs which are moulded on the inner surfaces of the pressure and suction side. The coolant exits from the vortex matrix into the flow path through 8 slotted windows near the trailing edge. In the front and middle inner channels there are ribs on the pressure and suction side walls to intensify convective cooling. The upper part of the vortex matrix is fed with coolant by means of additional openings from the middle channel. There are three vertical rows of holes near the leading edge of the blade to form a film cooling on the surface of the blade. The first row has 16 holes, the second and third rows have 17 holes each. All holes have a diameter of 0.55mm. The film cooling of the upper blade face is formed by blowing out a part of the coolant through four holes of 1 mm diameter on the peripheral end of the HPT RB.

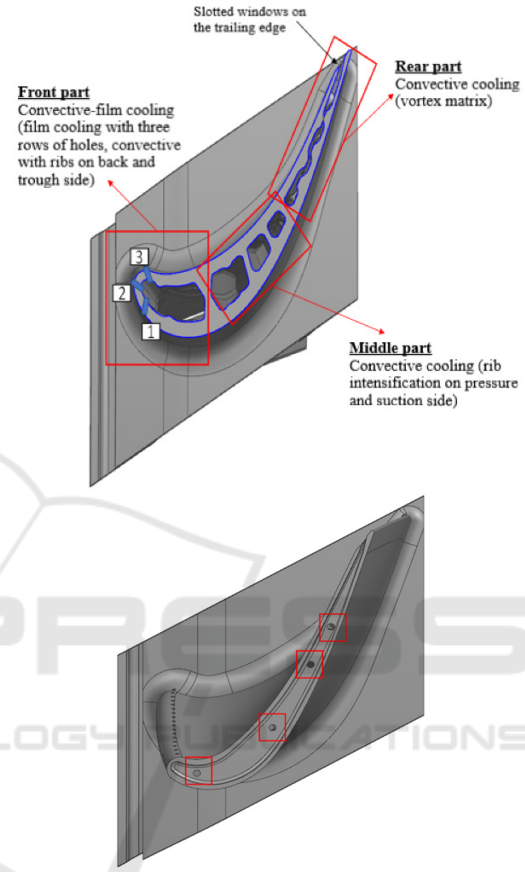

Figure 2: Blade cooling scheme, top view.

The computational model for the coupled thermal-hydraulic calculation of the RB was created in Ansys CFX (Ansys Workbench Product Release Notes). The CFD model of the RB consisted of four domains (Figure 3):

- the stationary domain of the NB blade passage channel;
- the rotating domain of the RW blade passage channel, also including the inter-disk cavity in front of and after the RW;
- rotating domain of the front, middle and rear parts of the inner cavity of the RW;
- the rotating domain of the cooling air inlet to the blade.
- Inlet 1 is the cross-section at the main flow inlet to the HPT;

- Inlet 2 - cross-section at the inlet to the RB cooling system;
- Inlet 3 - cross-section at the inlet to the cooling area of the front surface of the RW disc;
- Inlet 4 - cross-section at the inlet to the cooling area of the rear surface of the RW disc;
- Outlet - cross-section at the outlet of the main flow from the HPT.

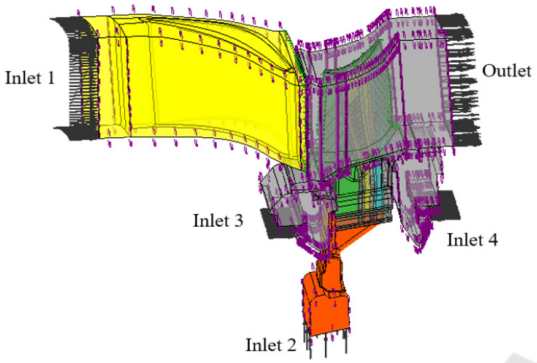

Figure 3: Computational model for coupled thermal-hydraulic calculation of the rotor blade.

The numerical values of the initial data were taken according to the results of the thermodynamic and hydraulic calculation of the engine, as well as the 1D calculation of the turbine.

The calculation took into account the fact that in the model there are 2 working bodies (air and combustion products), while taking into account that they depend on the gas temperature (Dorofeev V.M., 1973).

3 ANALYSIS OF BASIC ROTOR BLADE COOLING SCHEME

Figures 4 and 5 show calculated temperature distributions on external and internal surfaces of the rotor blade at cooling air flow rate G_{cool}= 4.2% of gas flow rate through throat of inter-blade channels of NB $G_{g.1NB}$.

The maximum value of the calculated RB temperature occurs in the periphery area closer to the trailing edge and is 1136.8 °C.

Figure 6 shows the distribution of temperature values and their average value in cross-sections located at different heights of the RB.

The maximum value of the calculated RB temperature occurs in the periphery area closer to the trailing edge and is 1136.8 °C./

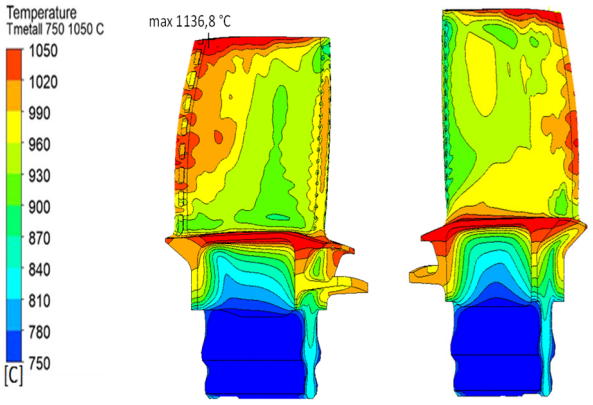

Figure 4: Temperature distribution on the external surfaces of the rotor blade.

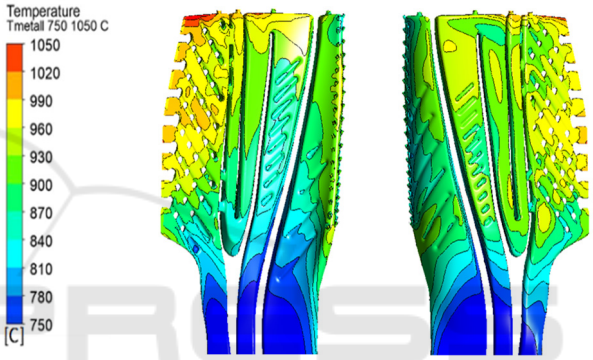

Figure 5: Temperature distribution on the internal surfaces of the rotor blade.

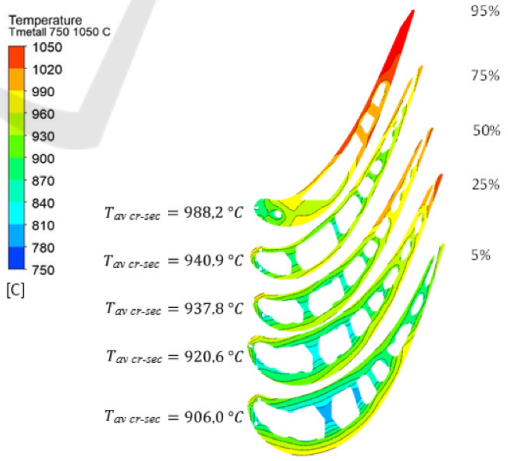

Figure 6: Shape of the basic rotor blade and its inner cavity.

Figure 6 shows the distribution of temperature values and their average value in cross-sections located at different heights of the RB.

Based on the obtained cross-sectional temperature distribution, the following problem areas were identified for the studied RB.

Firstly, it is the overheated peripheral part of the blade at the exit edge. And, secondly, there is an area with temperature difference more than 150°C from the middle of internal rib to the external surface of the suction side at the blade bottom (see Fig. 6, section at relative height from the hub equal to 5%). The presence of this zone leads to stresses that reduce the low-cycle fatigue margin.

Increased irregularity of the temperature field in the blade is caused by vortex zones and stagnation zones in the cooling channels. Examples are shown in Figures 7 and 8.

On the basis of the problems described, proposals have been developed for refining the internal cooling channels of the RB.

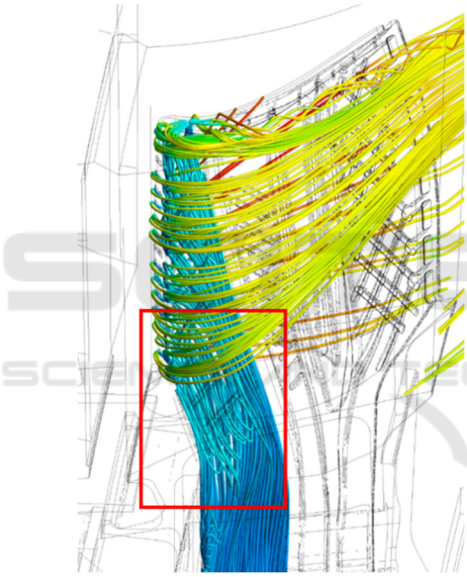

Figure 7: Vortex flow zone in the film cooling channel.

In order to eliminate the vortex in the film cooling channel, the shape of the channel was corrected, namely the ratio of the maximum cross-sectional area of the channel to the inlet cross-sectional area was reduced by a factor of 1.3. The cross-sectional areas of the film cooling channel have been modified as shown in Figures 9 and 10.

To reduce the blade temperature near the trailing edge, the shape of the internal channels was changed, through which air entered the matrix and was then discharged into the flow path of the turbine through the holes in the trailing edge. This also reduced hydraulic losses in the new channel configuration.

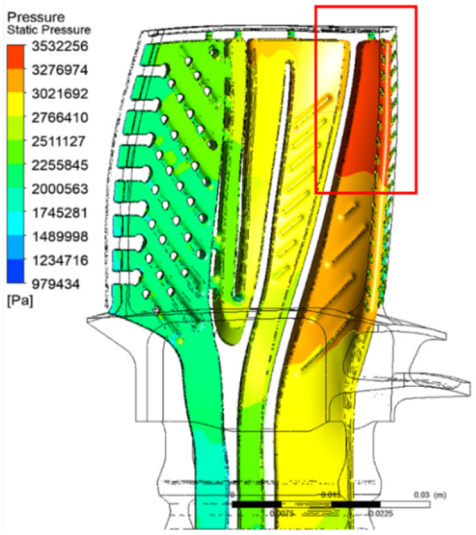

Figure 8: Stagnation zone in the film cooling channel.

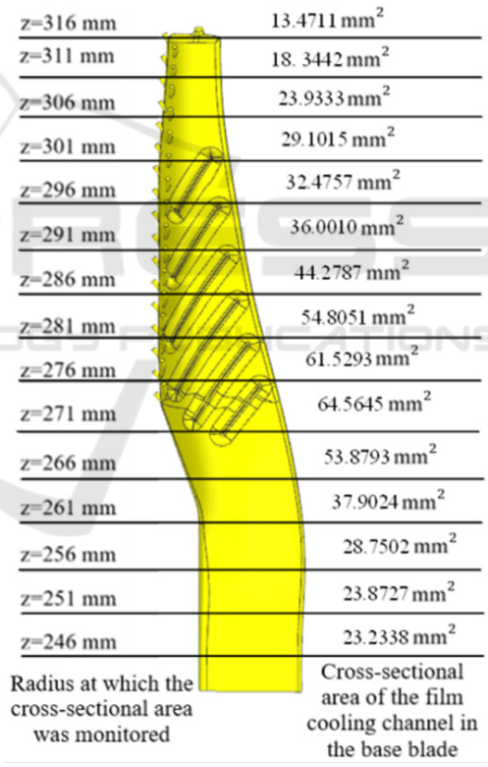

Figure 9: Cross-sectional areas of the film cooling channel of the basic scheme.

Connecting the film cooling channel to the vortex matrix channel helped to get rid of the stagnation zone and to additionally supply the overheated area around the trailing edge at the blade periphery with cooling air.

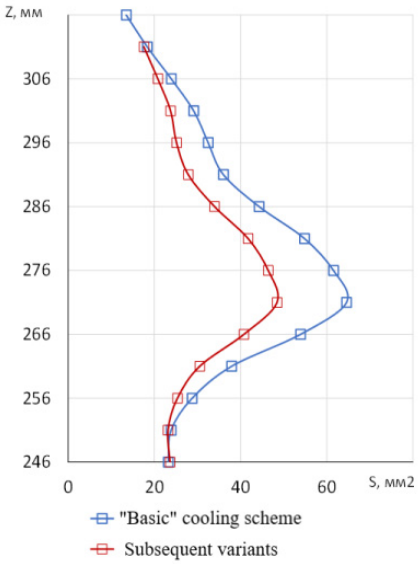

Figure 10: Change in cross-sectional area of the film cooling channel.

However, the film cooling operation was more difficult to regulate with this arrangement, because once all the channels were connected, the other two channels began to influence the film cooling parameters.

Also, to eliminate overheating near the trailing edge, the number of holes connecting the middle channel and the vortex matrix cavity was changed. Instead of five holes, unevenly spaced across the blade height, six holes were made without taking into account the overflow between the film cooling channel and the vortex matrix channel. In the new schemes, the holes were positioned directly opposite the openings in the trailing edge.

4 ANALYSIS OF NEW ROTOR BLADE COOLING SCHEMES

Figures 11 and 12 show the new cooling scheme variants, labelled "Variant 1" and "Variant 2".

For the "Variant 1" and "Variant 2" cooling schemes, calculations are performed at the same boundary conditions as for the blade with the basic internal cooling channel scheme.

Figures 13 and 14 shows distribution of cooling efficiency coefficient θ over blade height of all three schemes at cooling air flow rate G_{cool} = 4.2% of $G_{g.1NB}$.

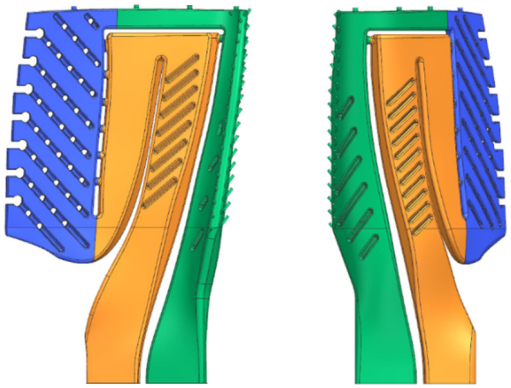

Figure 11: Cooling scheme "Variant 1".

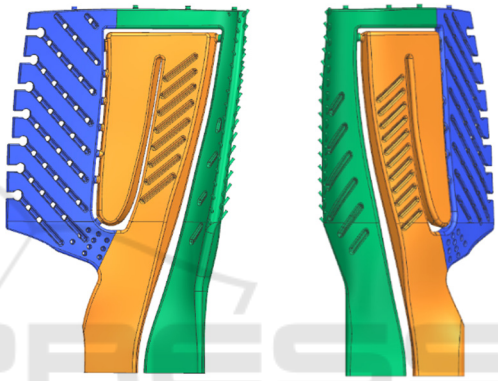

Figure 12: Cooling scheme "Variant 2".

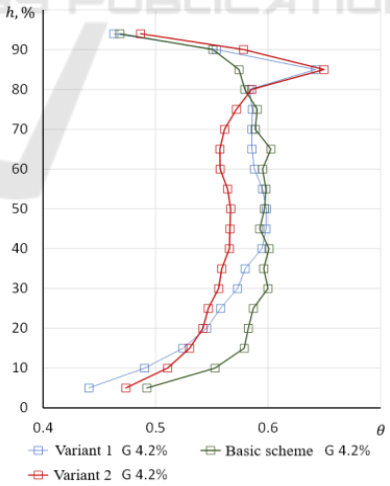

Figure 13: Comparison of cooling efficiency with different channel schemes.

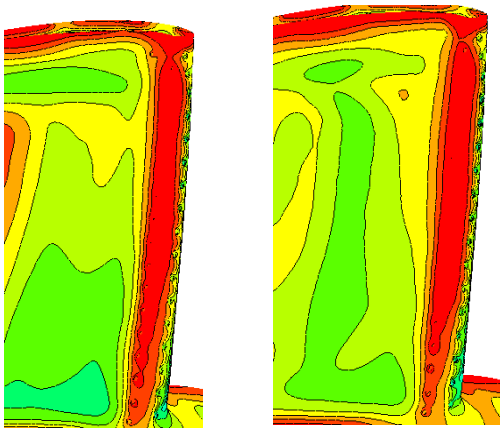

Figure 14: Temperature at leading edge of blades with hot air intake for "Variant 1" and "Variant 2" schemes.

Variant 1 performed better than the Variant 2. In Variant 2, due to the geometry of the channels, large vortex and stagnation zones were created, which were not supplied with cooling air. The vortex inside the cooling channels can be clearly seen in Figure 15. The part of the channel that was not receiving cooling air is also marked here. Therefore, for the subsequent improvement of the cooling channel system, the "Variant 1" scheme was selected.

The cross-sectional area of the channel connecting the film cooling cavity and the vortex matrix was halved to eliminate hot gas flowing into the blade's inner cavity in order to increase the static pressure in the film cooling cavity. The modified "Variant 1.2" cooling channel scheme is shown in Figure 16.

As can be seen from Figure 20, it was possible to significantly reduce the trailing edge temperature as a result of redistributing the cooling air flow in the vortex matrix.

Comparison of values of average cooling efficiency coefficient of "Variant 1" and "Variant 1.2" schemes by sections at different radii is shown in Figure 17, and distribution of θ by sections at different blade heights with "Variant 1.2" scheme is shown in Figure 18. For each blade section the cooling efficiency coefficient Θ_{cr-sec} was determined by the formula:

$$\Theta_{cr-sec} = \frac{T^*_{w\,gas} - T_{bl\,av\,in\,cr-sec}}{T^*_{w\,gas} - T^*_{w\,air}},$$

where $T^*_{w\,gas}$ is the total gas temperature in relative motion in front of the rotor blade at the corresponding radius;

$T^*_{w\,air}$ - total air temperature in relative motion at the inlet to the lower end of the rotor blade;

$T_{bl\,av\,in\,cr-sec}$ - average cross-sectional temperature of the blade.

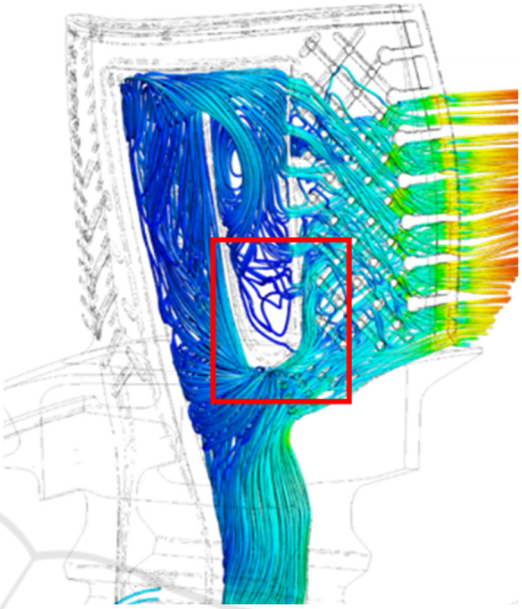

Figure 15: Area with insufficient cooling air.

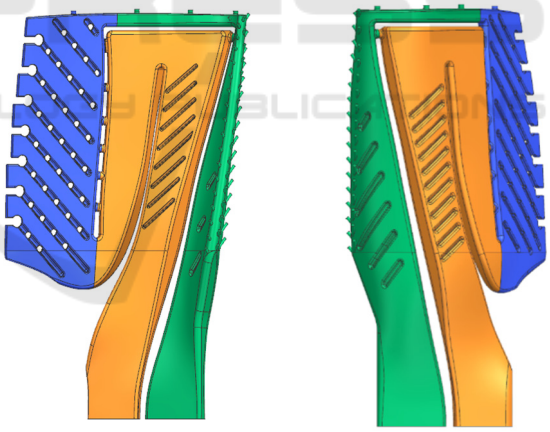

Figure 16: Cooling scheme "Variant 1.2".

As can be seen from the graphs in Figure 17, "Variant 1" has a higher cooling efficiency than "Variant 1.2" according to preliminary calculations. At the same time, the cooling efficiency of the two schemes is lower than that of the basic scheme. One of the reasons for this is that hot gas flows into the film cooling holes. This can be seen from the overheated leading edge in Figure 18.

Based on the data shown in the graphs in Figure 17, it can be concluded that the "Variant 1.2" scheme

is almost identical to the base one, in terms of integral values of section cooling efficiency at different radii.

Figure 19 shows a comparison of the blade temperature distributions over the cross-section at 5% of the airfoil height in the case of the base variant and "Variant 1.2". It can be seen that in the "Variant 1.2" scheme, the temperature gradient from the blade internal surfaces to the external one was reduced by changing the internal channel geometry.

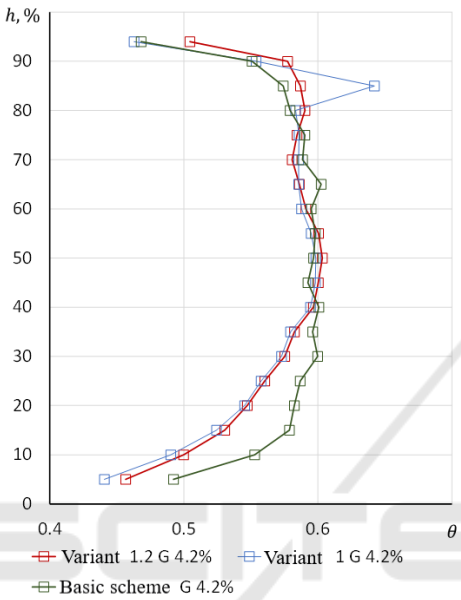

Figure 17: Distribution of θ by blade height for basic scheme and "Variant 1" and "Variant 1.2" schemes.

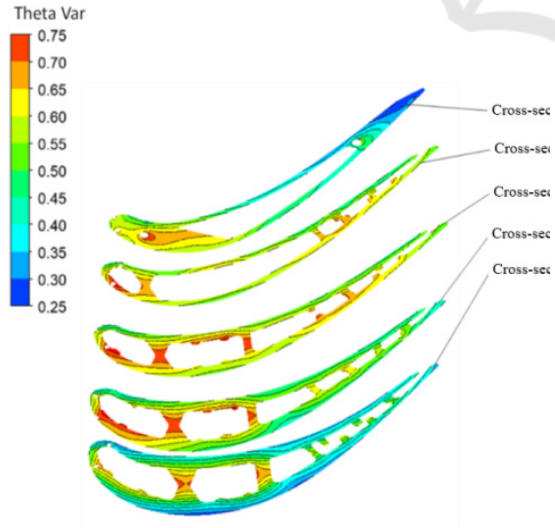

Figure 18: Distribution of θ across cross-sections at different blade heights "Variant 1.2" at cooling air flow rate G_{cool}= 4.2% of $G_{g.1NB}$.

A comparison of the temperature distribution over the blade surface with the basic scheme and with the "Variant 1.2" cooling scheme is shown in Figure 20. The "Variant 1.2" scheme has eliminated hot gas from entering the blade cooling system through the film cooling holes (see Figure 20, pressure side view of the "Variant 1.2" blade).

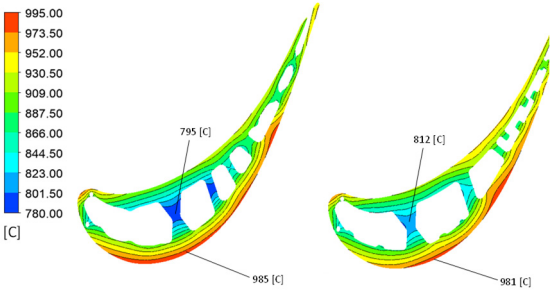

Base scheme. "Variant 1.2" scheme.

Figure 19: Comparison of the temperature distribution across the blade cross-section at 5% of blade height with the basic cooling scheme and with the "Variant 1.2" scheme.

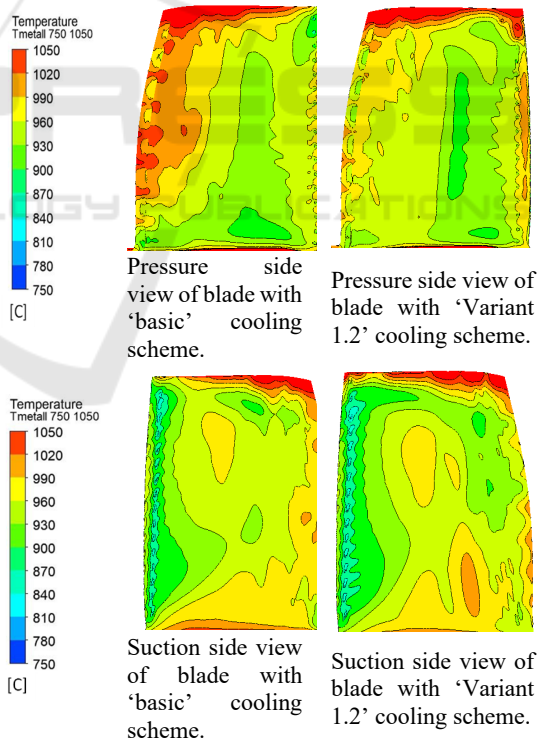

Pressure side view of blade with 'basic' cooling scheme.

Pressure side view of blade with 'Variant 1.2' cooling scheme.

Suction side view of blade with 'basic' cooling scheme.

Suction side view of blade with 'Variant 1.2' cooling scheme.

Figure 20: Temperature distribution over the blade surface with "basic" cooling scheme and "Variant 1.2" cooling scheme.

The leading edge of the blade with cooling scheme "Variant 1.2" is overheated in the periphery

area. This can be eliminated by changing the number and geometry of the film cooling holes in the problem area or by increasing the radius of the internal film cooling channel at its 90^0 turning point.

Also, as a result of changing the geometry of the cooling channels (as evidenced by the CFD calculation of the internal channels), an additional positive effect was obtained by reducing the total hydraulic resistance in the blade cavity by 116 kPa. This means that the same cooling air flow rate can be achieved at a lower pressure drop in the RB cooling scheme.

For all blade cooling schemes the values of cooling efficiency coefficient θ at different cooling air flow rates have been calculated. The results of these calculations are plotted on the general graph from study of Shevchenko M. I. (2017), see Figure 21. To be able to compare the calculated data with the graph, the values of θ have been recalculated using the temperature $T^*_{w\,air}$ at the inlet to the cooling cavity in the HPT disk, and the values of relative cooling air flow rate were recalculated depending on air flow rate at the inlet to the high pressure compressor of the designed engine.

5 CONCLUSIONS

The results of the analysis of the thermal-hydraulic calculation of the basic HPT rotor blade have been evaluated and the main directions of its refinement have been proposed, aimed at reducing the temperature of the trailing edge and the temperature difference between the external and internal surfaces of the blade.

A number of new blade cooling schemes based on the original geometric model have been developed. By comparing the results of conjugate modelling of the new blades with the initial data on the basic blade, the advantages and disadvantages of alternative schemes of internal cooling channels of the investigated RB were revealed.

The result is the "Variant 1.2" scheme, which eliminated the overheating of the trailing edge and reduced the temperature difference between the internal and external surfaces of the blade.
Therefore, the "Variant 1.2" scheme seems to be the most promising for further development. At the same time, the disadvantage of this scheme is difficulty of regulation of its operation in comparison with "basic" scheme, because all cavities inside the blade are connected with each other by means of special connection channels in the scheme "Variant 1.2".

In the future, with the help of the developed mathematical model, searches will be made for the shape of the internal channels of the blade, which will make it possible to obtain its best thermal state. In this case, rational convective cooling will be found at the first stage. Then the film cooling will be also modified.

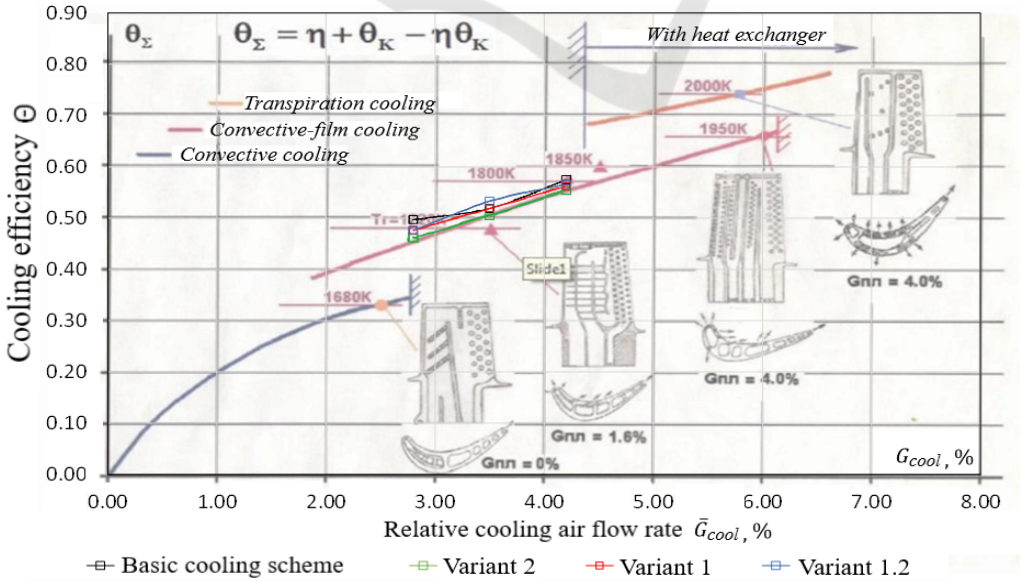

Figure 21: Comparison of the results of the calculation of the cooling efficiency of the rotor blades in question with the statistical data (Shevchenko M. I., 2017).

REFERENCES

Kopelev S. Z. (1983). *The tutorial*, Cooled blades of gas turbines. Thermal calculation and profiling. Nauka Publisher.

Nagoga G. P. (1996). *The tutorial*, Effective ways of cooling blades of high-temperature gas turbines. Moscow: MAI Publishing House.

Shevchenko M. I. (2017). *Dissertation*, Design of cooled GTE parts with advanced verification of thermal-hydraulic models by the example of cooled gas turbine blades.

Han J. C., Dutta S., Ekkad S. (2012). *The paper*, Gas Tubine Heat Transfer and Cooling Technology. Second Edition.

Vieser, W. (2002). *The paper*, Heat transfer prediction using advanced two-equation turbulence models.

Inozemtsev A. A., Sandratsky V.L. (2006). *The book*, Gas Turbine Engines.

Dorofeev V. M. (1973). *The book*, Thermogasodynamic Calculation of Gas Turbine Power Plants. Moscow, Mashinostroenie.

Ansys Workbench Product Release Notes. ANSYS, Inc. and ANSYS Europe, Ltd. are UL registered ISO 9001:2000 Companies.